Chemical Communications, issue 10, 2009, pp1273-1275

In situ antimony doping of solution-grown ZnO nanorods†

Joe Briscoe,* Diego E. Gallardo and Steve Dunn

Received (in Cambridge, UK) 20th November 2008, Accepted 24th December 2008
First published as an Advance Article on the web 19th January 2009
DOI: 10.1039/b820797f

ZnO nanorods are doped with Sb during the aqueous chemical synthesis by addition of Sb acetate dissolved in ethylene glycol.

The reliable production of p-type ZnO has been a challenge for some time. This is because the as-grown ZnO is nominally n-type due to intrinsic defects,[1] so holes introduced by acceptor dopants are generally compensated by the high intrinsic free electron density. Despite these difficulties, there have been increasing examples in recent years of p-type ZnO thin films and nanostructures. There is significant interest in producing p-type ZnO nanostructures due to many potential device applications. For example, transistors or diodes based on ZnO nano-homojunctions could be used for transparent electronics, UV optoelectronics and photonics.

In previous work on p-type ZnO nanostructures, acceptor dopants were generally introduced in gaseous form during high temperature growth or in post-growth annealing steps where nanorods were produced by low temperature processes. A method that introduces the dopant during low temperature synthesis would be attractive, as it would remove the need for high temperature annealing. In this paper, such a low-temperature method is presented. It is shown that by adapting established procedures for the chemical synthesis of ZnO nanorods, the acceptor dopant Sb can be incorporated into the nanorods in a single-step process, without the need for post-growth annealing.

Advances in the production of p-type ZnO have been made through doping with the group V elements N, P, As and Sb. Understanding acceptor doping by N and P is relatively simple as they substitute for oxygen, leading to the introduction of a shallow acceptor level. Acceptor doping with As and Sb in ZnO is slightly more complicated, as their larger ionic radii mean that it is very energetically unfavourable for them to substitute for oxygen. However, it was shown that doping ZnO with these elements did produce p-type thin films.[1] This behaviour was explained by Limpijumnong *et al.* to result from the formation of the complex $As/Sb_{Zn}–2V_{Zn}$ (As or Sb on a zinc site coupled to two zinc vacancies), which was shown to be a shallow acceptor.[2] The experimental success coupled with theoretical explanation meant that many more p-type ZnO thin films were produced, including those doped with As or Sb.[3–5] These films were produced by high energy, high vacuum growth methods such as molecular-beam epitaxy or pulsed laser deposition where the dopant was introduced to the growth source(s).

To produce ZnO nanostructures, growth methods generally fall into two main categories: vapour-phase or aqueous chemical. Addition of the group V acceptor dopants during vapour-phase synthesis of ZnO nanorods is achieved by introducing either gaseous (N or P) or vaporised (As or Sb) dopants to the synthesis. These methods have been shown to produce doped ZnO nanostructures that exhibit p-type behaviour.[6–8] Compared to vapour-phase methods, aqueous chemical synthesis routes are attractive because they use much lower temperatures (<100 °C), which makes them lower-cost synthesis methods and also compatible with polymer substrates. As mentioned, in the previous attempts to make p-type ZnO by chemical methods, the dopants were added using post-growth steps such as annealing in the presence of N-containing gases,[6] or sources of As.[7] These methods require the introduction of a high temperature annealing step, which eliminates the advantages gained by using chemical synthesis methods.

The substrates used in this study were indium–tin oxide (ITO) coated glass onto which a layer of silver was deposited by thermal evaporation. Nanorods were then grown hydrothermally by immersing these substrates into a solution of zinc nitrate and hexamethylenetetramine (HMT) and heating to 90 °C for two hours in a sealed container, which led to nanorod growth perpendicularly from the Ag substrate. The reactant concentration was varied to alter the size of the nanorods;[9] an equimolar, 0.01 M solution was used to produce small nanorods (100 nm across, 500 nm long), and a 0.1 M solution was used to produce much larger rods (1 μm across, 5 μm long). These are shown in Fig. 1.

The rods were doped with Sb by adding Sb acetate to the reaction in proportions of 5, 1 or 0.1 at.%. This was either added directly to the reaction bath or dissolved in ethylene glycol (EG) and then added as a solution. The Sb acetate in EG solutions were produced so that when added to the reaction the concentration of EG in the final solution was

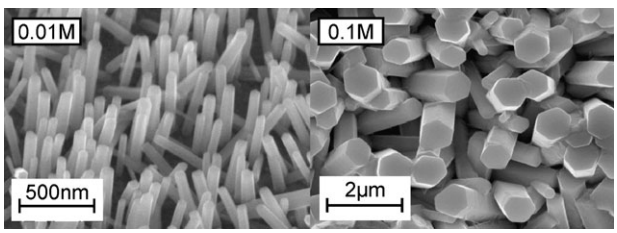

Fig. 1 SEM images of undoped ZnO nanorods grown hydrothermally on Ag-coated substrates in equimolar solutions of zinc nitrate and HMT at either 0.01 M or 0.1 M as indicated.

Microsystems and Nanotechnology Centre, Cranfield University, Bedford, UK MK43 0AL. E-mail: j.briscoe@cranfield.ac.uk; Fax: +44 (0)1234 751346; Tel: +44 (0)1234 754066

† Electronic supplementary information (ESI) available: XRD patterns of samples with all Sb contents produced; UV-Vis absorption spectra. See DOI: 10.1039/b820797f

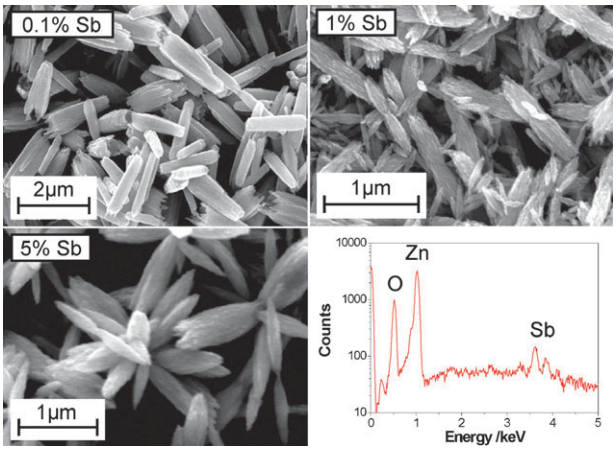

Fig. 2 SEM images of ZnO nanorods doped with indicated quantities of Sb. Doping was achieved by adding Sb acetate directly to the chemical bath containing 0.01 M zinc nitrate and HMT. Few nanorods were nucleated on the substrates, so the rods shown are those that grew homogeneously in solution, which were washed and deposited for imaging. EDX spectrum shows that Sb is clearly detected in 5 at.% doped rods.

0.36 M and the Sb ion concentration was 5, 1 or 0.1% that of the zinc ions. In both cases, ZnO nanostructures were still produced, and the Sb content was confirmed by EDX spectroscopy (Fig. 2) to be 0.22,‡ 0.66 and 2.49 at.% Sb when 0.1, 1 and 5 at.% Sb was added to the reaction. When Sb acetate was added directly to the reaction, the crystal quality of the rods was strongly affected, which led to ovoid structures (Fig. 2). When Sb acetate was dissolved in EG before adding to the reaction solution, there was a much less marked effect on the nanorod growth, as can be seen in Fig. 3. The rods retain the hexagonal structure of ZnO, and nucleate well on the substrate. They do have a slightly higher aspect ratio compared to undoped rods (Fig. 1), and are also smaller. Control experiments adding only EG to the reaction without Sb acetate showed that the EG did not have a noticeable effect on the reaction when added on its own.

To ensure Sb had actually been incorporated into the rods, EDX scans were performed on isolated rods, which had been suspended in solution and repeatedly washed to remove possible traces of chemicals used in the synthesis. An example EDX spectrum is shown in Fig. 3, and the inset to the

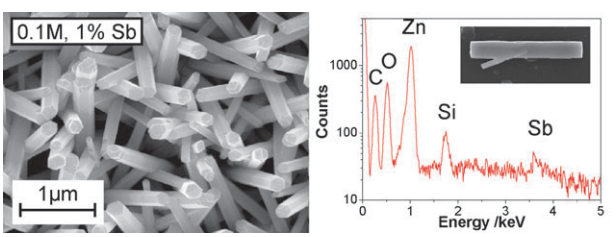

Fig. 3 SEM images of ZnO nanorods doped with 1 at.% Sb acetate, initially dissolved in ethylene glycol. EDX spectrum of a rod grown by the same method. Sb is detected along with Zn and O from the rod. Si and C are from the substrate. Inset shows a typical rod (~5 μm long), which was washed to remove trace chemicals and deposited on carbon-coated glass.

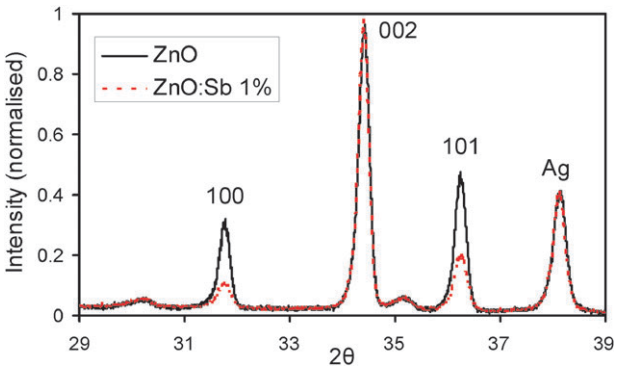

Fig. 4 X-Ray diffraction patterns of undoped and doped rods, as shown in Fig. 1 and 3, normalised to the 002 peak and overlaid for comparison. The peak from the Ag substrate can also be seen in both spectra†.

spectrum shows the rod that was surveyed. A survey of 45 points detected an average of 0.66 ± 0.08 at.% Sb.

As the SEM analysis suggests that using Sb acetate dissolved in EG does not significantly alter the morphology of the nanorods, X-ray diffraction measurements were performed to ascertain the structure of the rods (Fig. 4). These show that both undoped and 1 at.% Sb-doped nanorods with EG in the reaction have the wurzite structure of ZnO. The high 002 peak is indicative of nanorods that are elongated along the *c*-axis, and the relative height of this peak is even more pronounced in the Sb-doped rods, which correlates with the higher aspect ratio observed in the SEM images (Fig. 3).

To explain the role of EG in the successful *in situ* Sb-doping of ZnO nanorods, it is necessary to consider the chelating effect of EG. When dissolved directly in water, Sb acetate can readily react to directly form Sb_2O_3.[10] It is therefore likely that Sb is incorporated into the ZnO nanorods as ready-formed particles of Sb_2O_3, which would significantly disrupt the nanorod growth as observed, acting as irregular nucleation points for the nanorod growth. When the Sb acetate is dissolved in EG, the EG will act as a chelating ligand for the Sb ions in the solution. When this solution is added to the aqueous bath, the formation of Sb_2O_3 is inhibited. This means that Sb ions, not Sb_2O_3, will be supplied directly to the reaction, and will take up lattice positions within the ZnO structure. The effect of EG is therefore to control the supply of Sb ions to the reaction in a similar way that HMT controls the free Zn ion concentration.[11]

To probe the effect of Sb-doping on the defect chemistry of the ZnO nanorods, photoluminescence (PL) measurements were performed. The spectra were recorded by measuring the emitted spectrum from the undoped and doped nanorod arrays when illuminated with 266 nm light from a frequency quadrupled Nd:YAG laser. The region of the exciton peak of ZnO is shown in Fig. 5 for both undoped and 0.1 at.% Sb-doped ZnO, which have been normalised to the highest peaks. The spectrum for undoped ZnO clearly shows the exciton peak at 385 nm, which also has slight shoulders at higher wavelengths, particularly at 400 nm. The main difference in the spectrum for 0.1 at.% Sb-doped ZnO is that the emission at 400 nm has become much more pronounced. A peak at 400 nm has been observed previously in ZnO spectra

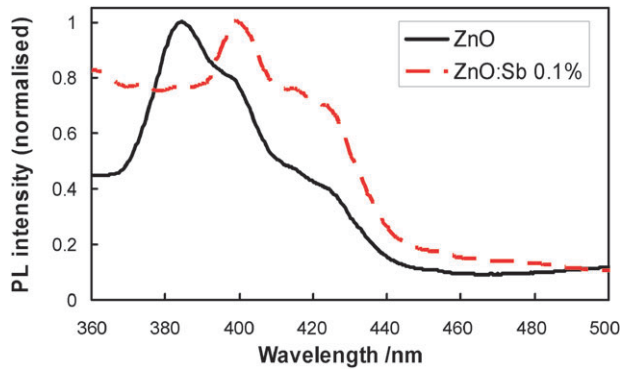

Fig. 5 Photoluminescence spectrum of undoped and Sb-doped ZnO nanorods normalised to spectral maxima.

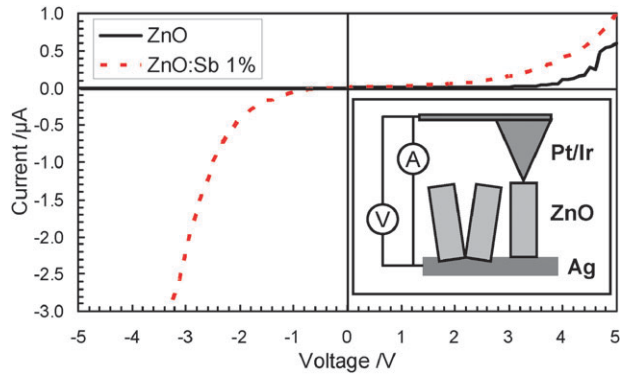

Fig. 6 Current–voltage characteristics of an undoped and a 1 at.% Sb-doped nanorod. Inset shows schematic of AFM apparatus.

and has been associated with zinc vacancies (V_{Zn}), normally occurring in the surface.[12,13] When observed in Sb-doped samples, the spectral evidence of increased V_{Zn} content suggests that the defect complex Sb_{Zn}–$2V_{Zn}$ has been produced. Yang *et al.* also observed a lower energy peak in Sb-doped ZnO compared to undoped, attributing this to an increase in band tailing.[14] However, this could equally be attributed to emission from defect levels introduced by Sb combined with complete suppression of the original exciton emission.

To investigate the effect of Sb-doping on the electrical properties of the nanorods, current–voltage measurements were performed on both the doped and the undoped nanorods. These were taken using an atomic force microscope (AFM) fitted with a Pt–Ir tip. The tip of the AFM was lowered onto the top of a nanorod, a voltage was applied between the AFM tip and the Ag substrate, and the resultant current was measured. The applied voltage range was ±5 V, equivalent to ±1 MV m^{-1} for a rod length of 5 μm. The forward current (positive voltages) corresponds to positive Pt and negative Ag. The resulting current–voltage data are shown in Fig. 6, with a schematic of the set-up shown in the inset.

In the undoped case, the *I–V* curve shows no significant reverse current. The forward current switches on at about 4.0 V, with exponential growth. These results indicate the existence of two opposing Schottky diodes at the interfaces of the nanorod and the metals. The absence of reverse current indicates that the potential barrier for electrons is larger for the Pt contact, which can be explained by its higher work function with respect to Ag. The behaviour is consistent with the expected band configuration of n-type nanorods, and the current is due exclusively to electrons.

In the Sb-doped case, the forward current switches on around +2.0 V, with an exponential growth. The reverse current switches on around −1.0 V and shows non-linear behaviour that does not fit a single model. This behaviour is similar to previous *I–V* measurements on acceptor-doped ZnO,[15] although these use a variety of different structures for measurements, which makes direct comparison difficult. The overall behaviour in the Sb-doped case is consistent with a model based on p-type nanorods with a Fermi level near the valence band. However, this behaviour could also be explained by electron currents assisted by defect states. Further analysis is necessary for a more complete understanding.

In conclusion, it has been shown that Sb can be incorporated into ZnO nanorods during their chemical growth procedure by adding Sb acetate to the reaction. By dissolving the Sb acetate in ethylene glycol before the reaction, Sb can be incorporated into the ZnO nanorods without adversely affecting the nanorod morphology and structure. Initial electrical characterisation of the nanorods shows that the addition of Sb to the rods leads to a large change in the electrical transport characteristics, and photoluminescence measurements show a high level of zinc vacancies in the doped nanorods, which are associated with p-type behaviour.

We would like to thank Steve James, Edmond Chehura and Sammy Cheung for the use of and help with their Nd:YAG laser. This work was funded by EPSRC grant number EP/P503507/1.

Notes and references

‡ Sb content detected was greater than that added when 0.1 at.% was added to the reaction, which seems implausible. However, this quantity is near to the detection limit of the EDX, so this value may be exaggerated.

1 T. Aoki, Y. Shimizu, A. Miyake, A. Nakamura, Y. Nakanishi and Y. Hatanaka, *Phys. Status Solidi B*, 2002, **229**, 911.
2 S. Limpijumnong, S. B. Zhang, S. H. Wei and C. H. Park, *Phys. Rev. Lett.*, 2004, **92**, 155504-1.
3 F. X. Xiu, Z. Yang, L. J. Mandalapu, D. T. Zhao, J. L. Liu and W. P. Beyermann, *Appl. Phys. Lett.*, 2005, **87**, 152101.
4 H. S. Kang, G. H. Kim, D. L. Kim, H. W. Chang, B. D. Ahn and S. Y. Lee, *Appl. Phys. Lett.*, 2006, **89**, 181103.
5 W. Guo, A. Allenic, Y. B. Chen, X. Q. Pan, Y. Che, Z. D. Hu and B. Liu, *Appl. Phys. Lett.*, 2007, **90**, 242108.
6 C. C. Lin, H. P. Chen and S. Y. Chen, *Chem. Phys. Lett.*, 2005, **404**, 30.
7 M. Sun, Q. F. Zhang and J. L. Wu, *J. Phys. D: Appl. Phys.*, 2007, **40**, 3798.
8 B. Xiang, P. Wang, X. Zhang, S. A. Dayeh, D. P. R. Aplin, C. Soci, D. Yu and D. Wang, *Nano Lett.*, 2007, **7**, 323.
9 L. Vayssieres, *Adv. Mater.*, 2003, **15**, 464.
10 P. Christian and P. O'Brien, *J. Mater. Chem.*, 2005, **15**, 4949.
11 K. Govender, D. S. Boyle, P. B. Kenway and P. O'Brien, *J. Mater. Chem.*, 2004, **14**, 2575.
12 X. L. Wu, G. G. Siu, C. L. Fu and H. C. Ong, *Appl. Phys. Lett.*, 2001, **78**, 2285.
13 Z. Wang, B. Huang, X. Liu, X. Qin, X. Zhang, J. Wei, P. Wang, S. Yao, Q. Zhang and X. Jing, *Mater. Lett.*, 2008, **62**, 2637–2639.
14 Y. Yang, J. Qi, Q. Liao, Y. Zhang, L. Tang and Z. Qin, *J. Phys. Chem. C*, 2008, **112**, 17916–17919.
15 L. J. Mandalapu, F. X. Xiu, Z. Yang and J. L. Liu, *J. Appl. Phys.*, 2007, **102**, 023716.